

# Density functional studies of magneto-optic properties of $\text{Sr}_2\text{GdReO}_6$

Saadi Berri<sup>1</sup>, Sabah Chami<sup>2</sup>, Mourad Attallah<sup>3</sup>, Mouloud Oumertem<sup>4</sup>, Djamel Maouche<sup>1</sup>

<sup>1</sup> Laboratory for Developing New Materials and their Characterizations, University of Setif 1, Algeria

<sup>2</sup> Laboratory of Electro-Mechanic Systems (LASEM), National School of Engineers of Sfax (ENIS) University of Sfax, Sfax, Tunisia

<sup>3</sup> Department of Physics, Faculty of Sciences, University of Biskra, Algeria

<sup>4</sup> Department of Physics, Faculty of Sciences, University of Msila, Algeria

Corresponding author: Saadi Berri (berrisaadi12@yahoo.fr)

Received 13 October 2017 ♦ Accepted 5 January 2018 ♦ Published 1 May 2018

**Citation:** Berri S, Chami S, Attallah M, Oumertem M, Maouche D (2018) Density functional studies of magneto-optic properties of  $\text{Sr}_2\text{GdReO}_6$ . Modern Electronic Materials 4(1): 13–19. <https://doi.org/10.3897/j.moem.4.1.31135>

## Abstract

The electronic structure and magneto-optic properties of the  $\text{Sr}_2\text{GdReO}_6$  double perovskite were investigated using the full-potential linearized augmented plane wave (FPLAPW) method. Exchange correlation effects are treated using the generalized gradient approximations GGA, GGA +  $U$  and GGA +  $U$  + SOC approaches. At ambient conditions, these calculation predict a half-metallic character for  $\text{Sr}_2\text{GdReO}_6$  material. The electronic band structures and density of states demonstrate that  $\text{Sr}_2\text{GdReO}_6$  is HM with a magnetic moment of  $9 \mu_B/\text{f.u.}$  and HM flip gap of 1.82 eV. The half metallicity is attributed by the double-exchange interaction mechanism via the  $\text{Gd}(4f)\text{--O}(2p)\text{--Re}(t_{2g})$   $\pi$ -bonding. These new double perovskite may become ideal candidate material for future spintronic applications. The analysis charge densities show that bonding character as a mixture of covalent and ionic nature. The optical properties are analyzed and the origin of some peaks in the spectra is described. Besides, the dielectric function  $\epsilon(\omega)$ , refractive index  $n(\omega)$  and extinction coefficient  $K(\omega)$  for radiation up to 14 eV have also been reported.

## Keywords

Double perovskite, Half-metallic, Magnetic properties, Optical properties, Electronic structure

## 1. Introduction

Many works have been focused on the double-perovskite structure with different compositions and structures because of to their possible applications in numerous industrial and engineering domains [1–5]. These compounds have many interesting properties such as tunnelling magnetoresistance [6], colossal magnetoresistance [7], ferromagnetism [8, 9], magneto-optic properties [10], metallicity [11], multiferroicity [12] and magnetodielectric properties [13]. The observation of high magneto-re-

sistance in half-metallic for Sr-based double perovskite with fairly high transition temperature [14] of 410 K indicates the promise in double perovskite materials as candidates for high temperature half metallic magnets [15].

Many double-perovskite compounds are found to possess the half-metallic band structure as revealed by the ab-initio calculations [16–22]. Samanta et al. [23] calculated the electronic structures and magnetic properties of  $\text{Sr}_2\text{CrOsO}_6$  using full-potential linearized augmented plane wave (FPLAPW) scheme within the (GGA) +  $U$ . Jeng and Guo [24] calculated magnetic and electronic

structure of Sr<sub>2</sub>FeMoO<sub>6</sub>, Sr<sub>2</sub>FeReO<sub>6</sub>, and Sr<sub>2</sub>CrWO<sub>6</sub> using full-potential linear muffin-tin orbital method within the GGA +  $U$  and LSDA +  $U$  methods. The electronic structure calculations predicted a HMF band structure with spin magnetic moment of  $4\mu_B$ ,  $3\mu_B$ , and  $2\mu_B$  per formula unit for Sr<sub>2</sub>FeMoO<sub>6</sub>, Sr<sub>2</sub>FeReO<sub>6</sub>, and Sr<sub>2</sub>CrWO<sub>6</sub>, respectively. Faizan *et al.* [25], also predicted that Sr<sub>2</sub>XOsO<sub>6</sub> ( $X = \text{Li, Na, Ca}$ ) were HM ferromagnets. The electronic structure calculations predicted a HMF band structure for Sr<sub>2</sub>XOsO<sub>6</sub> ( $X = \text{Li, Na, Ca}$ ), with energies band gap of 1.90, 1.83 and 2.24 eV for Sr<sub>2</sub>LiOsO<sub>6</sub>, Na and Ca respectively. The structural and electronic properties have been investigated at zero and elevated pressure for the double perovskite Sr<sub>2</sub>GdReO<sub>6</sub> using the density functional theory (GGA) +  $U$  approach [26].

In the present paper, the magnetic, electronic and optical properties of Sr<sub>2</sub>GdReO<sub>6</sub> are reported. As far as the electronic structure and optical properties of materials are concerned, these features play a crucial role in determining their magneto-optic properties for devices. Therefore, accurate knowledge of these properties is very important for the application. The aim of this work is to examine the electronic band structure of Sr<sub>2</sub>GdReO<sub>6</sub>, with emphasis on its derived properties. The calculations are performed using *ab initio* a full relativistic version of the full-potential augmented plane-wave scheme within GGA and GGA +  $U$  approaches. The rest of the paper is organized as follows: The theoretical background is presented in Section 2. Results and discussions are presented in Section 3. A summary of the results is given in Section 4.

## 2. Method of calculations

For the present computational study, we have considered the experimental crystal parameters [27] as reported by Baud and Capestan. Sr<sub>2</sub>GdReO<sub>6</sub> crystallizes in the ( $Fm3m$  cubic space group), with  $Z = 4$  formula unit

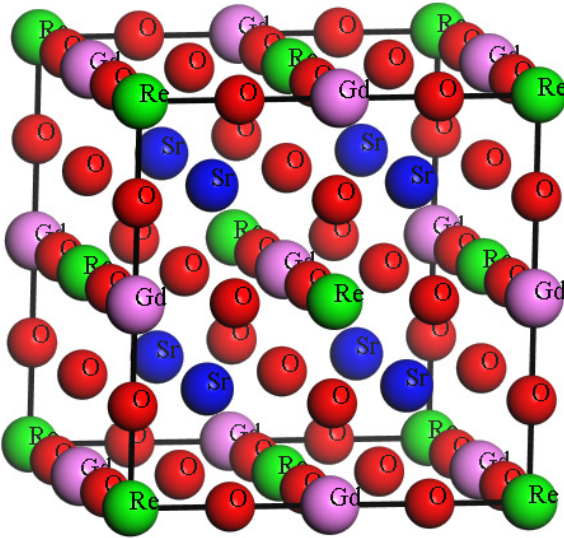


**Figure 1.** The crystal structures of Sr<sub>2</sub>GdReO<sub>6</sub> compound.

per unit cell having a lattice parameters of 8.279 Å. The Wyckoff positions of atoms with an occupancy of 1 are as follows: Sr 8c (0.25, 0.25, 0.25), Gd 4b (0.5, 0.5, 0.5), Re 4a (0, 0, 0) and O 24e (0.25, 0, 0). The crystal structures of these compounds are shown in Fig. 1. We have used the full-potential linearized augmented plane wave (FP-LAPW) and local orbitals method through a density functional theory approach [28, 29]. Here, the Kohn–Sham equations are solved by expanding the wave functions in the spherical harmonics form inside the atom spheres. Plane wave expansion is used in the interstitial regions of atoms inside the unit cell. We have used  $l_{\max} = 10$  for angular momentum expansion and  $R_{\text{MT}}K_{\max} = 8$  as a plane wave cut-off with 2000 k points to achieve self-consistency. Here  $R_{\text{MT}}$  is the average muffin-tin (MT) radius and  $K_{\max}$  is the wave function cut-off. The radii  $R_{\text{MT}}$  of the muffin tins (MT) are chosen to be approximately proportional to the corresponding ionic radii. The energy between successive iterations is converged to 0.0001 Ry and forces are minimized to 1 mRy Bohr<sup>-1</sup>. The Monkhorst–Pack (MP) technique is used for Brillouin zone integrations. Exchange-correlation effects are treated using generalized gradient approximation (GGA) as parameterized by Perdew *et al.* [30] and GGA +  $U$  by Anisimov *et al.* [31] with an approximate correction for the self-interaction correction. This is probably best suited for our system and for a full potential method we use an effective  $U_{\text{eff}} = U + J$ , setting  $J = 0.5$  and  $U = 7.4$  eV, for Gd atoms and  $J = 0.3$ ,  $U = 3$  eV for Re atoms quoted from Refs. [32] and [33], respectively. To treat the interactions of heavier elements like Gd and Re one needs to consider SOC during the calculations. A dense k-mesh with 5000 k-points was used in the first Brillouin zone to calculate the linear optical properties.

Optical properties of a solid are usually described in terms of the complex dielectric function  $\epsilon(\omega) = \epsilon_1(\omega) + i\epsilon_2(\omega)$ . The imaginary part  $\epsilon_2(\omega)$  was calculated from the momentum matrix elements between the occupied and unoccupied wave functions within the selection rules. The real part  $\epsilon_1(\omega)$  of the dielectric function was calculated by the Kramer–Kronig transformation [34] of the imaginary part  $\epsilon_2(\omega)$ . Other optical constants were computed from the values of  $\epsilon(\omega)$ . The frequency dependent complex dielectric tensor  $\epsilon_2(\omega)$  components are calculated by using the following mathematical expressions [35]:

$$\epsilon_2(\omega) = \frac{16\pi e^2}{\omega^2} \sum_s \bar{\lambda} \langle O | \text{vec}v | s \rangle^2 \delta(\omega - \Omega^2) \quad (1)$$

$$\epsilon_1(\omega) = 1 + \frac{2P}{\pi} \int_0^\infty \sum \frac{\omega' \epsilon_2(\omega')^2}{\omega'^2 - \omega^2} d\omega' \quad (2)$$

where  $\bar{\lambda}$  is the polarization vector of light.  $\langle O | \text{vec}v | s \rangle$  is the optical transition matrix from valence to conduction states and  $P$  is the principal value of the integral and the integral is over irreducible Brillouin zone. The optical constants such as refractive index  $n(\omega)$  and the extinction coefficient  $k(\omega)$ , are calculated in terms of the real and

the imaginary parts of the complex dielectric function as follows [36]:

$$n(\omega) = \frac{\left[ \varepsilon_1(\omega) + \left( \varepsilon_1^2(\omega) + \varepsilon_2^2(\omega) \right)^{\frac{1}{2}} \right]^{\frac{1}{2}}}{\sqrt{2}} \quad (3)$$

$$k(\omega) = \frac{\left[ -\varepsilon_1(\omega) + \left( \varepsilon_1^2(\omega) + \varepsilon_2^2(\omega) \right)^{\frac{1}{2}} \right]^{\frac{1}{2}}}{\sqrt{2}} \quad (4)$$

### 3. Results and discussion

As presented in Fig. 2, the electronic properties of the  $\text{Sr}_2\text{GdReO}_6$  compound are assessed the band structures, total and partial densities of states of Gd  $f$ , Re  $e_g$  and  $t_{2g}$ , Sr  $e_g$  and  $t_{2g}$  and O  $p_z$  and  $d$  electrons in FM phase. Note that the density of states was presented only for GGA +  $U$  method because it is similar to that of GGA and GGA +  $U$  + SOC method with a small difference. It is clear that the majority-spin band is metallic, while the minority spin band shows a semiconducting gap around the Fermi level. The energy band gap ( $E_{g\downarrow} = 2.02$  eV) in spin down channel is formed by the nonbonding states Re  $4d$  of the conduction band and the bonding states O  $p$  of valence band. The present study show that the energy gap for spin-down electrons for  $\text{Sr}_2\text{GdReO}_6$  compound is 2.02 eV, and close to the energy gap values for the  $\text{La}_2\text{CrZnO}_6$  compound [37]. This energy gap in the minority-spin band gap leads to 100% spin polarization at the Fermi level, resulting in the half-metallic behavior at equilibrium state.

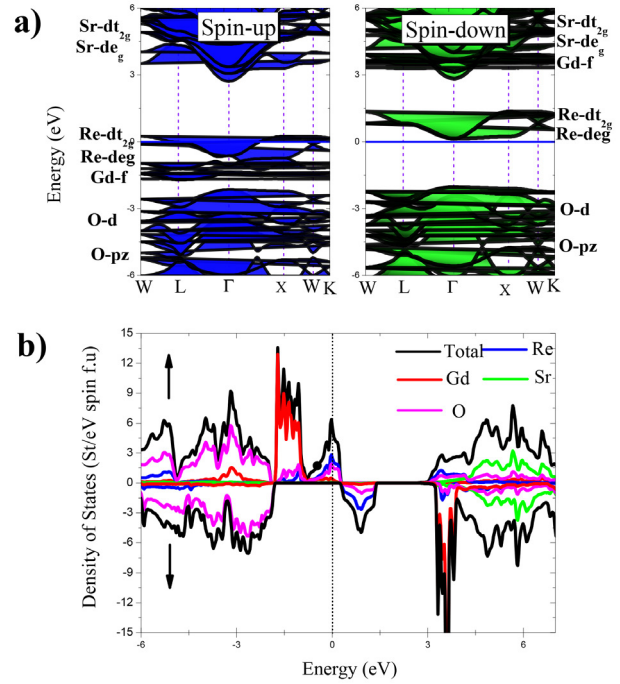


**Figure 2.** Spin-polarized a) band structure, partial and b) total densities of states (TDOS) of  $\text{Sr}_2\text{GdReO}_6$  compound.

We have calculated the band structure along symmetry directions in the first Brillouin zone with/without SOC and this is shown in Fig. 3. Note that, there is an overall topological resemblance for  $\text{Sr}_2\text{GdReO}_6$  compound for both methods.

The half-metallic gap [38, 39], which is determined as the minimum between the lowest energy of majority (minority) spin conduction bands with respect to the Fer-

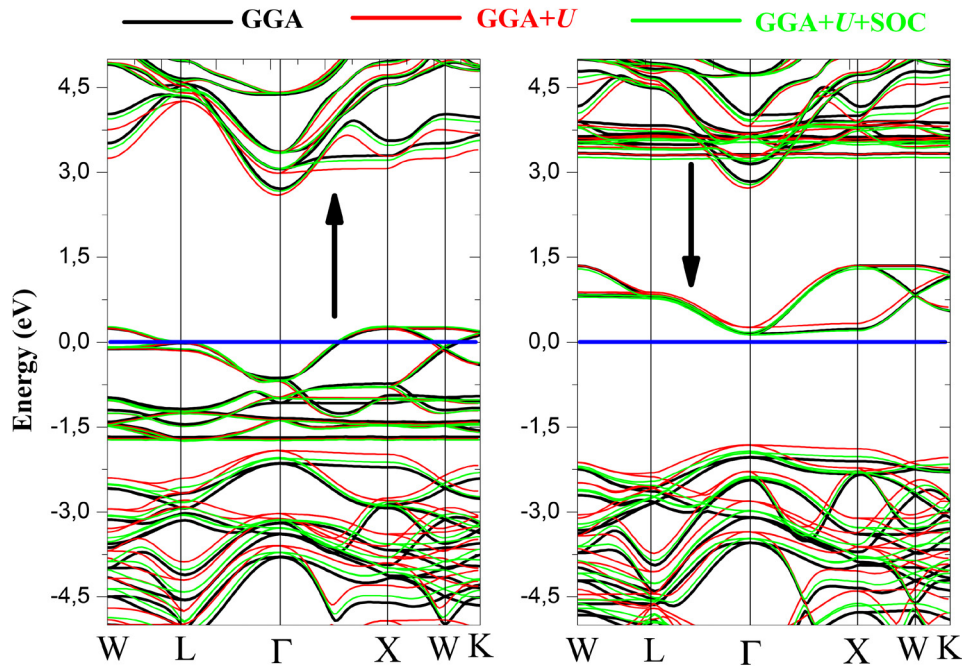


**Figure 3.** The calculated band structure for GGA, GGA +  $U$  and GGA +  $U$  + SOC of  $\text{Sr}_2\text{GdReO}_6$  compound.

mi level and the absolute values of the highest energy of the majority (minority) spin valence bands, is 1.82 eV, for both method.

The hybridisation bonding states  $p_z$  and  $d$  electrons of O element (See Fig. 2a), which contribute to the TDOS in the energy region from  $-8.0$  to  $-2.0$  eV for both spin channels, are mainly formed by Gd- $4f$  and  $t_{2g}$  states of Re atoms creates fully occupied bands with a positive spin-splitting (the exchange-splitting between the spin-up and spin-down sub-bands of the Gd  $4f$  states is approximately 4.75 eV, which is the main contributor in the magnetic moment of these compound).

For unoccupied states of both spin channels above the Fermi level, the nonbonding hybridisation state in spin-down channel of TDOS is  $4F$ -Gd and  $e_g$  electron of Re atoms situated in the range from 0.5 to 4.0 eV, and the  $e_g$  and  $t_{2g}$  states of Sr atoms contribute to the majority and minority spin states mix with  $e_g$  electron of Re atom in the region from 4.0 to 8.0 eV.

The calculated total and atom-resolved magnetic moments, using GGA, GGA +  $U$  and GGA +  $U$  + SOC for  $\text{Sr}_2\text{GdReO}_6$  compound, are summarized in Table 1. The present study shows that the total magnetic moment for  $\text{Sr}_2\text{GdReO}_6$  compound is  $\approx 9 \mu_B/\text{fu}$  for both approximations. Here, the main contribution to the total magnetic moment is due to Gadolinium and Rhenium atom, and the magnetic moment on the Strontium and Oxygen atoms are small. Our results for magnetic moment for Gadolinium atoms which is in agreement with previous studies

[40, 41]. The magnetic moments of the Rhenium atoms are in agreement with theoretical data [42].

Normally, exchange interactions are very short-ranged, confined to electrons in orbitals on the same atom or nearest neighbor atoms but longer-ranged interactions can occur via intermediary atoms and this is termed superexchange. The double-exchange mechanism is a type of a magnetic exchange that may arise between ions in different oxidation states. First proposed by Clarence Zener [43] and later developed by Anderson and Hasegawa [44], by Kubo and Ohata [45] and by Furukawa [46], is generally agreed to provide a description of the FM ground state this theory predicts the relative ease with which an electron may be exchanged between two species. Electronic structures from a full-potential linearized augmented plane wave method also demonstrated that the half-metallic character is not caused by direct Gd-Gd or Re-Re interactions but by indirect O-Gd-O-Re  $p$ - $f$  and  $\pi$ - $d$  couplings, which are simulate ane ously responsible for their ferrimagnetic character [46].

In order to understand the nature of chemical bonding, we display, in Fig. 4 the contours of charge densities in (110) plane for  $\text{Sr}_2\text{GdReO}_6$  compound. From Fig. 4, we can see that the near spherical charge distribution around the Sr atoms site is negligible and as a result the bonding Sb-O has expected to be some ionic character. On an other hand, the O atoms hybridization with Gd and Re atoms for spin-up and spin-down (See Fig. 2a), happen with an interaction

**Table 1.** The calculated total and partial magnetic moment (in  $\mu_B$ ) for  $\text{Sr}_2\text{GdReO}_6$  compound.

	$m_{\text{Gd}}$	$m_{\text{Re}}$	$m_{\text{Sr}}$	$m_{\text{O}}$	$m_{\text{interstitial}}$	$m_{\text{Total}}$
GGA	6.72563	1.31451	0.0088	0.04382	0.67677	9.00
GGA + $U$	6.75414	1.34922	0.0072	0.03992	0.64067	9.00
GGA + $U$ + SOC	6.77910	1.33155	0.0070	0.04507	0.62448	9.00

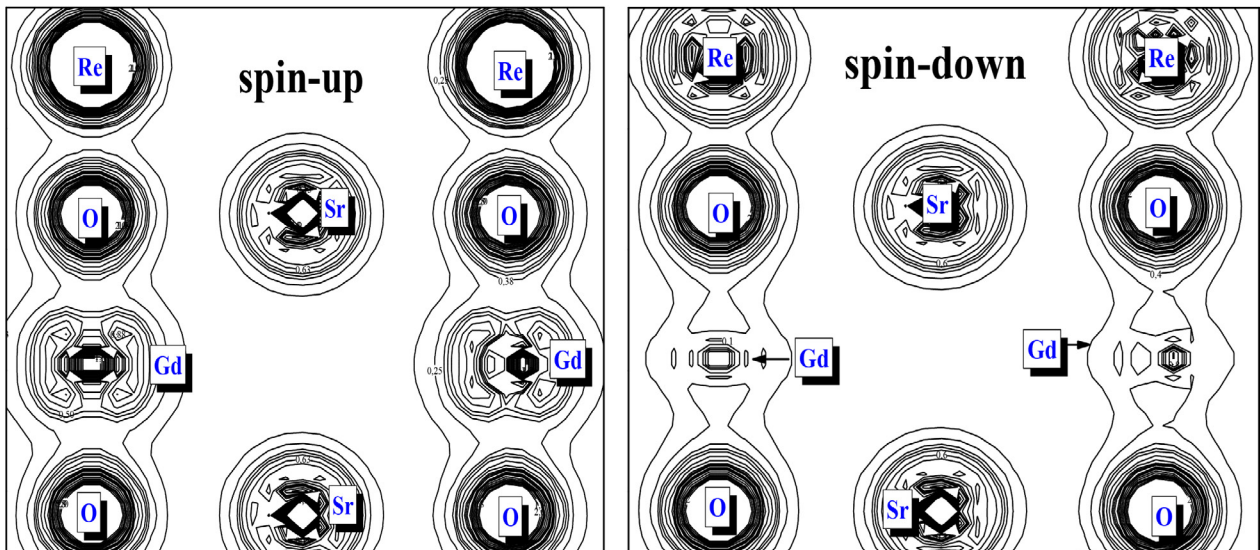


**Figure 4.** Charge density distribution in the plane (110) of  $\text{Sr}_2\text{GdReO}_6$  compound.

between the Gd and Re with O atom, indicating that a covalent interaction occurs between Gd and Re with O atoms. The bonding character may be described as a mixture of covalent and ionic character. To our knowledge, there are no experimental or theoretical data reported for the electronic structure for the material of interest, and hence our results are predictions.

Magneto-optical effects comprise various changes in the polarization state if light upon interaction with materials possessing a net magnetic moment, including rotation of the plane of linearly polarized light (Faraday, Kerr rotation), and the complementary differential absorption of left and right circularly polarized light (circular dichroism) [47].

Mainly, the first Microscopic dielectric function describes the behaviour of linear response of a material to the electromagnetic radiation field applied which displays the absorptive character of that material. The real part of the dielectric function describes how much material polarized as a result of induced electric dipole creation when an electric field is applied while the imaginary part indicates how much material absorption photon energy. There are two contributions to  $\epsilon_2(\omega)$ , namely, intraband and interband transitions. The contribution from intraband transitions is important only for metals. The interband transitions can further be split in to direct and indirect transitions. We neglect the indirect interband transitions, which involve scattering of phonons and are expected to give only a small contribution to  $\epsilon_2(\omega)$ .

In Fig. 5a we present the dielectric function of  $\text{Sr}_2\text{GdReO}_6$  as calculated by FP-LAPW method. For energies up to 14 eV, based on our calculated band structure it would be worthwhile to identify the interband transitions that are responsible for the structure in  $\epsilon_2(\omega)$ . Our analysis of the  $\epsilon_2(\omega)$  spectra shows that the threshold energy (first critical point) of the dielectric function occurs at about 2.39, 2.62 and 3.83 eV, respectively. These points are mainly coming from the electron transition from the Gd 4*f* (VB), O-*d*(VB) and O-*pz*(VB) to Re  $t_{2g}$  (CB) orbitals. We note that in  $\text{Sr}_2\text{GdReO}_6$  compound,  $\epsilon_2(\omega)$  shows peaks located at 6.64 eV and 7.51 eV, respectively. This point is mainly derived from the transition from Gd 4*f*(VB) and O-*d*(VB) to Sr  $t_{2g}$  (CB) orbitals. The behaviour of  $\epsilon_1(\omega)$  (See Fig. 5b) seems to be rather similar to that of  $\epsilon_2(\omega)$ . Below the reststrahlen region in the optical spectra, the real part of the dielectric function asymptotically approaches the static or low-frequency dielectric constant  $\epsilon_0$ , in the present contribution, the calculated static dielectric constant  $\epsilon_0$  for spin-down is 2.93 for  $\text{Sr}_2\text{GdReO}_6$  compound.

The refractive index is a quantity that describes how much light is refracted after entering material [48, 49]. The calculated refractive index  $n(\omega)$  and the extinction coefficient  $k(\omega)$  using GGA approach are displayed in Fig 5 (c and d). From the refractive index plot, we remark that the material possesses high refractive index within Infrared region and decreases at higher energy in the Ultraviolet lountain. Note that in this compound the extinction coefficient has resonance in the low energy

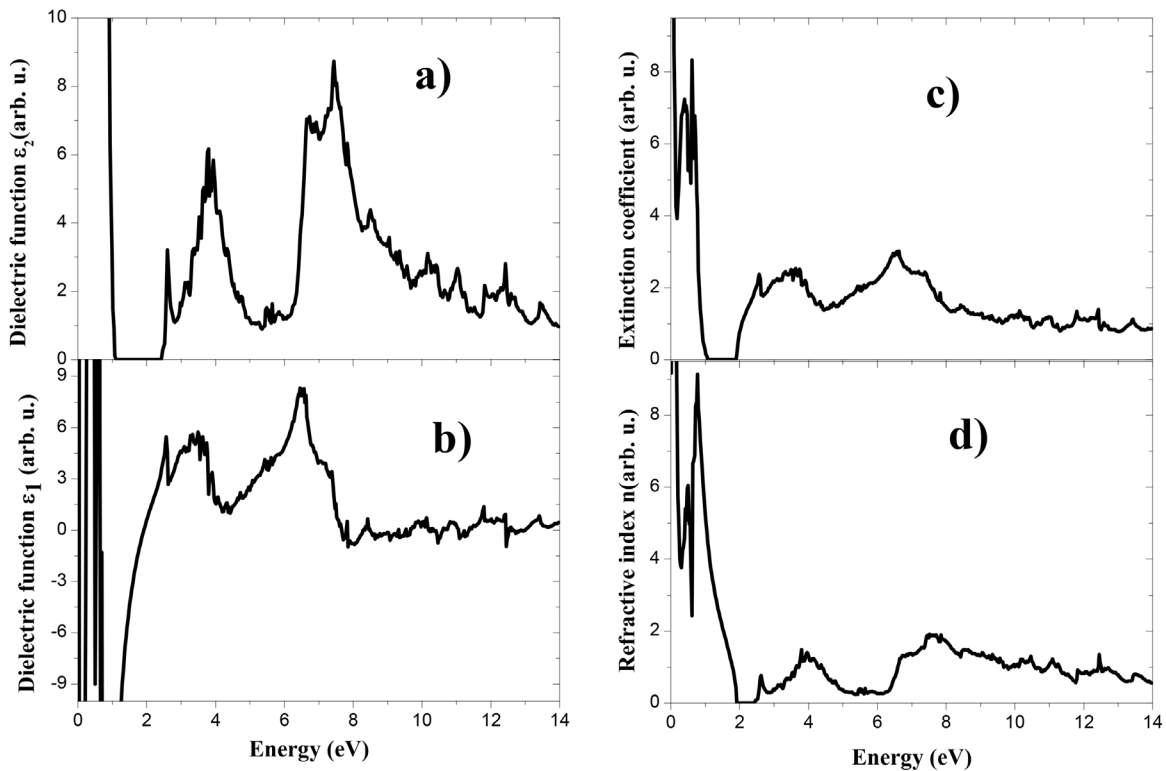


**Figure 5.** The calculated a) real parts of dielectric function, b) imaginary parts of dielectric function, c) refractive index and d) extinction coefficient.

region. Our results of  $k(\omega)$  show that Sr<sub>2</sub>GdReO<sub>6</sub> has strong extinction effects at Infrared region and then decreases with photon energy forming the maximum peak at 0.8 eV. In the absence of both experimental and theoretical data of the dielectric function, refractive index and extinction coefficients for the material of interest, to the best of our knowledge, no comment can be ascribed to used method and hence our results may serve only for a reference.

## 4. Conclusion

For the Sr<sub>2</sub>GdReO<sub>6</sub> compound, The electronic structure and magneto-optic properties the electronic structure

and magnetic has been studied by using first-principle FPLAPW calculation method..At ambient conditions, these calculation predict a half-metallic character for Sr<sub>2</sub>GdReO<sub>6</sub> material. The electronic band structures and density of states demonstrate that Sr<sub>2</sub>GdReO<sub>6</sub> is HM with a magnetic moment of 9  $\mu_B$ /fu and HM flip gap of 1.82 eV. The half metallicity is attributed by the double-exchange interaction mechanism via the Gd(4f)–O(2p)–Re( $t_{2g}$ )  $\pi$ -bonding. The analysis of charge densities contours leads us to conclude that the bonding character in Sr<sub>2</sub>GdReO<sub>6</sub> compound is a mixture between covalent and ionic nature. To complete the fundamental characteristics of this compound we have analyzed their optical properties such as the dynamic dielectric function, refractive index, extinction coefficient for a wide range of 0–14 eV.

## References

- Anderson M.T., Greenwood K.B., Taylor G.A., Poeppelmeier K.R. B-cation arrangements in double perovskites. *Progress in Solid State Chemistry*. 1993; 22: 197–233. [https://doi.org/10.1016/0079-6786\(93\)90004-B](https://doi.org/10.1016/0079-6786(93)90004-B)
- Borges R.P., Thomas R.M., Cullinan C., Coey J.M.D., Suryanarayanan R., Ben-Dor L., Pinsard-Gaudart L., Revcolevschi A. Magnetic properties of the double perovskites A<sub>2</sub>FeMoO<sub>6</sub>; A = Ca, Sr, Ba. *J. Phys.: Condens. Matter*. 1999; 11(40): L445. <https://doi.org/10.1088/0953-8984/11/40/104>
- Ritter C., Ibarra M. R., Morellon L., Blasco J., García J., De Teresa J.M. Structural and magnetic properties of double perovskites AA'FeMoO<sub>6</sub> (AA' = Ba<sub>2</sub>, BaSr, Sr<sub>2</sub> and Ca<sub>2</sub>). *J. Phys.: Condens. Matter*. 2000; 12(38): 8295. <https://doi.org/10.1088/0953-8984/12/38/306>
- García-Hernández M., Martínez J.L., Martínez-Lope M.J., Casais M.T., Alonso J.A. Finding Universal Correlations between Cationic Disorder and Low Field Magnetoresistance in FeMo Double Perovskite Series. *Phys. Rev. Lett*. 2001; 86: 2443. <https://doi.org/10.1103/PhysRevLett.86.2443>
- Huang Y.-H., Dass R.I., Xing Z.-L., Goodenough J.B. Double Perovskites as Anode Materials for Solid-Oxide Fuel Cells. *Science*. 2006; 312(5771): 254–257. <https://doi.org/10.1126/science.1125877>
- Arulraj A., Ramesha K., Gopalakrishnan J., Rao C.N.R. Magnetoresistance in the Double Perovskite Sr<sub>2</sub>CrMoO<sub>6</sub>. *J. Solid State Chemistry*. 2000; 155(1): 233–237. <https://doi.org/10.1006/jssc.2000.8939>
- Kobayashi K.I., Kimura T., Tomioka Y., Sawada H., Terakura K., Tokura K. Intergrain tunneling magnetoresistance in polycrystals of the ordered double perovskite Sr<sub>2</sub>FeReO<sub>6</sub>. *Physical Review B*. 1999; 59: 11159. <https://doi.org/10.1103/PhysRevB.59.11159>
- Fuh H.R., Liu Y.P., Xiao Z.R., Wang Y.K. New type of ferromagnetic insulator: Double perovskite La<sub>2</sub>NiMO<sub>6</sub> (M = Mn, Tc, Re, Ti, Zr, and Hf). *J. Magnetism and Magnetic Materials*. 2014; 357: 7–12. <https://doi.org/10.1016/j.jmmm.2013.12.049>
- Carvajal E., Navarro O., Allub R., Avignon M., Alasc B. Electronic properties of double perovskite compounds. *Phys. Status Solidi (b)*. 2005; 242(9):1942–1945. <https://doi.org/10.1002/pssb.200461726>
- Das H., De Raychaudhury M., Saha-Dasgupta T. Moderate to large magneto-optical signals in high Tc double perovskites. *Appl. Phys. Lett*. 2008; 92: 201912. <https://doi.org/10.1063/1.2936304>
- Kato H., Okuda T., Okimoto Y., Tomioka Y., Takenoya Y., Ohkubo A., Kawasaki M., Tokura Y. Metallic ordered double-perovskite Sr<sub>2</sub>CrReO<sub>6</sub> with maximal Curie temperature of 635 K. *Appl. Phys. Lett*. 2002; 81: 328. <https://doi.org/10.1063/1.1493646>
- Azuma M., Takata K., Saito T., Ishiwata S., Shimakawa Y., Takano M. Designed Ferromagnetic, Ferroelectric Bi<sub>2</sub>NiMnO<sub>6</sub>. *J. Am. Chem. Soc*. 2005; 127: 8889. <https://doi.org/10.1021/ja0512576>
- Rogado N.S., Li J., Sleight A.W., Subramanian M.A. Magnetocapacitance and Magnetoresistance Near Room Temperature in a Ferromagnetic Semiconductor: La<sub>2</sub>NiMnO<sub>6</sub>. *Adv. Mater. (Weinheim, Ger.)*. 2005; 17: 2225. <https://doi.org/10.1002/adma.200500737>
- Kobayashi K.-I., Kimura T., Sawada H., Terakura K., Tokura Y. Room-temperature magnetoresistance in an oxide material with an ordered double-perovskite structure. *Nature*. 1998; 395: 677. <https://doi.org/10.1038/27167>
- Coey J.M.D. Materials for Spin Electronics. In *Lecture Notes in Physics* 569, (eds Thornton M. J. & Ziese M.), Ch. 12, 277–297 (Springer, Berlin, New York, 2001). [https://doi.org/10.1007/3-540-45258-3\\_12](https://doi.org/10.1007/3-540-45258-3_12)
- Yan Zhang , Li Duan, Vincent Ji, The half-metallic ferromagnetic characters of (001)-oriented thin films of the double perovskite Pb<sub>2</sub>FeMoO<sub>6</sub>. *Thin Solid Films*. 2016; 615: 318–323. <https://doi.org/10.1016/j.tsf.2016.07.042>
- Liu Y.P., Fuh H.R., Wang Y.K. Expansion research on half-metallic materials in double perovskites of Sr<sub>2</sub>BB'O<sub>6</sub> (B = Co, Cu, and Ni; B' = Mo, W, Tc, and Re; and BB' = FeTc). *Comput. Mater. Sci*. 2014; 92: 63–68. <https://doi.org/10.1016/j.commatsci.2014.05.013>
- Liu Y.P., Fuh H.R., Xiao Z.R., Wang Y.K. Theoretical prediction of half-metallic materials in double perovskites Sr<sub>2</sub>Cr(Co)B'O<sub>6</sub> (B' = Y, La, Zr, and Hf) and Sr<sub>2</sub>V(Fe)B'O<sub>6</sub> (B' = Zr and Hf). *J. Alloys Compd*. 2014; 586: 289–294. <https://doi.org/10.1016/j.jallcom.2013.10.043>
- Haiping Wu, Yan Qian, Weishi Tan, Erjun Kan, Ruifeng Lu, Kaiming Deng, Vacancy-induced insulator – direct spin gapless semiconductor – half-metal transition in double perovskite La<sub>2</sub>CrFeO<sub>6</sub>: A first-principles study. *Physics Letters A*, 2015;379(43–44):2897–2901. <https://doi.org/10.1016/j.physleta.2015.09.028>
- Chuanyun Xiao, Kaiming Deng, The effect of oxygen vacancy on the half-metallic nature of double perovskite Sr<sub>2</sub>FeMoO<sub>6</sub>: A theoret

- ical study. *Solid State Communications*. 2014; 177: 57–60. <https://doi.org/10.1016/j.ssc.2013.09.029>
21. Liu Y.P., Fuh H.R., Wang Y.K. Study of the half-metallic materials double perovskites  $\text{Sr}_2\text{ZnBO}_6$  (B = Tc, Re, Ru, Os, Co, Pd, and Au) via first-principle calculations. *J. Magn. Magn. Mater.* 2013; 341: 25–29. <https://doi.org/10.1016/j.jmmm.2013.04.023>
  22. Jing Wang, Jian-Min Zhang, Su-Fang Wang, Ke-Wei Xu. First-principles study on the half-metallic Tc-doped  $\text{Sr}_2\text{FeReO}_6$ . *J. Magn. Magn. Mater.* 2013; 329: 30–33. <https://doi.org/10.1016/j.jmmm.2012.10.020>
  23. Kartik Samanta, Prabuddha Sanyal and Tanusri Saha-Dasgupta, Half-Metallic Behavior in Doped  $\text{Sr}_2\text{CrOsO}_6$  Double Perovskite with High Transition Temperature. *Sci. Rep.* 2015; 5: 15010. <https://doi.org/10.1038/srep15010>
  24. Jeng H.-T., Guo G.Y. First-principles investigations of orbital magnetic moments and electronic structures of the double perovskites  $\text{Sr}_2\text{FeMoO}_6$ ,  $\text{Sr}_2\text{FeReO}_6$ , and  $\text{Sr}_2\text{CrWO}_6$ . *Physical Review B*. 2003; 67: 094438. <http://dx.doi.org/10.1103/PhysRevB.67.094438>
  25. Faizan M., Murtaza G., Khan S.H., Khan A., Mehmood A., Khenata R., Hussain S. First-principles study of the double perovskites  $\text{Sr}_2\text{XOsO}_6$  (X = Li, Na, Ca) for spintronics applications. *Bulletin of Materials Science*. 2016; 39(6): 1419–1425. <https://doi.org/10.1007/s12034-016-1288-6>
  26. Berri S. First-principles study on half-metallic properties of the  $\text{Sr}_2\text{GdReO}_6$  double perovskite. *J. Magn. Magn. Mater.* 2015; 385: 124–128. <https://doi.org/10.1016/j.jmmm.2015.03.025>
  27. Baud G., Capestan M. Sur des oxydes ternaires de structure Perovskite contenant du rhenium pentavalent. *Bulletin de la Societe Chimique de France*. 1969;3608–3612.
  28. Blaha P., Schwarz K., Madsen G.K.H., Kvasnicka D., Luitz J. WIEN2K, an Augmented Plane Wave + Local orbitals program for calculating crystal properties (Karlheinz Schwarz, Technische Universität, Wien, Austria, 2001), ISBN 3-9501031-1-2.
  29. Slater J.C. Atomic Radii in Crystals. *The Journal of Chemical Physics*. 1964; 41(10): 3199. <https://doi.org/10.1063/1.1725697>
  30. Perdew J.P., Burke S., Ernzerhof M. Generalized Gradient Approximation Made Simple. *Phys. Rev. Lett.* 1996; 77: 3865. <https://doi.org/10.1103/PhysRevLett.77.3865>
  31. Anisimov V.I., Zaanen J., Andersen O.K. Band theory and Mott insulators: Hubbard  $U$  instead of Stoner  $I$ . *Phys. Rev. B: Condens Matter*. 1991; 44(3): 943–954. <https://doi.org/10.1103/PhysRevB.44.943>
  32. Ioannis Bantounas, Souraya Goumri-Said, Mohammed Benali Kanoun, Aurélien Manchon, Iman Roqan, Udo Schwingenschlögl. *Ab initio* investigation on the magnetic ordering in Gd doped ZnO. *J. Appl. Phys.* 2011; 109(8): 083929. <https://doi.org/10.1063/1.3574924>
  33. Gao H., Llobet A., Barth J., Winterlik J., Felser C., Panthöfer M., Tremel W. Structure-property relations in the distorted ordered double perovskite  $\text{Sr}_2\text{InReO}_6$ . *Phys. Rev. B*. 2011; 83: 134406. <https://doi.org/10.1103/PhysRevB.83.134406>
  34. Alouani M., Wills J.M. Calculated optical properties of Si, Ge, and GaAs under hydrostatic pressure *Physical Review B*. 1996; 54: 2480. <https://doi.org/10.1103/PhysRevB.54.2480>
  35. Reshak A.H., Auluck S. Electronic and optical properties of the 1T structures of  $\text{TiS}_2$ ,  $\text{TiSe}_2$  and  $\text{TiTe}_2$ . *Phys Rev B*. 2003; 68: 245113. <https://doi.org/10.1103/PhysRevB.68.245113>
  36. Delin A., Eriksson A.O., Ahuja R., Johansson B., Brooks M.S., Gasche T., Auluck S., Wills J.M. Optical properties of the group-IVB refractory metal compounds. *Phys. Rev. B*. 1996; 54:1673. <https://doi.org/10.1103/PhysRevB.54.1673>
  37. Liu Y.P., Chen S.H., Fuh H.R., Wang Y.K. First-Principle Calculations of Half-Metallic Double Perovskite  $\text{La}_2\text{BB}'\text{O}_6$  (B, B' = 3d transition metal). *Commun. Comput. Phys.* 2013; 14: 174–185. <https://doi.org/10.4208/cicp.190312.190712a>
  38. Xu Y.-Q., Liu B.-G., Pettifor D.G. Half-metallic ferromagnetism of MnBi in the zinc-blende structure. *Physical Review B*. 2002; 66: 184435. [https://doi.org/10.1016/S0921-4526\(02\)02464-X](https://doi.org/10.1016/S0921-4526(02)02464-X)
  39. Liu B.-G. Robust half-metallic ferromagnetism in zinc-blende CrSb. *Physical Review B*. 2003; 67: 172411. <https://doi.org/10.1103/PhysRevB.67.172411>
  40. Antic B., Mitric M., Rodic D., Zhong Y., Artemov Y., Bogdanovich S., Friedman J.R. Magnetic properties of diluted magnetic  $(\text{Gd,Lu})_2\text{O}_3$ . *Physical Review B*. 1998; 58: 3212–3217. <https://doi.org/10.1103/PhysRevB.58.3212>
  41. Berri S., Maouche D., Zerarga F., Medkour Y. Ab initio study of the structural, electronic, elastic and magnetic properties of  $\text{Cu}_2\text{GdIn}$ ,  $\text{Ag}_2\text{GdIn}$  and  $\text{Au}_2\text{GdIn}$ . *Physica B*. 2012; 407: 3328–3334. <https://doi.org/10.1016/j.physb.2012.04.012>
  42. Wang Y.K., Guo G.Y. Robust half-metallic antiferromagnets  $\text{LaAVO}_6$  and  $\text{LaAMoYO}_6$  (A = Ca, Sr, Ba; Y = Re, Tc) from first-principles calculations. *Physical Review B*. 2006; 73: 064424. <https://doi.org/10.1103/PhysRevB.73.064424>
  43. Zener C. Interaction between the d-Shells in the Transition Metals. II. Ferromagnetic Compounds of Manganese with Perovskite Structure. *Physical Review*. 1951; 82: 403. <https://doi.org/10.1103/PhysRev.82.403>
  44. Anderson P.W., Hasegawa H. Considerations on Double Exchange. *Physical Review*. 1955; 100: 675. <https://doi.org/10.1103/PhysRev.100.675>
  45. Kubo K., Ohata N. A Quantum Theory of Double Exchange. I. *J. Phys. Soc. Jpn.* 1972; 33: 21–32. <https://doi.org/10.1143/JPSJ.33.21>
  46. de Gennes P.-G. Effects of Double Exchange in Magnetic Crystals. *Physical Review*. 1960; 118: 141. <https://doi.org/10.1103/PhysRev.118.141>
  47. Graf T., Felser C., Parkin S.S.P. Simple rules for the understanding of Heusler compounds. *Progress in Solid State Chemistry*. 2011; 39(1): 1-50. <https://doi.org/10.1016/j.progsolidstchem.2011.02.001>
  48. Lawal A., Shaari A., Ahmed R., Jarkoni N.  $\text{Sb}_2\text{Te}_3$  crystal a potential absorber material for broadband photodetector: A first-principles study. *Results in Physics*. 2017; 7: 2302–2310. <https://doi.org/10.1016/j.rinp.2017.06.040>
  49. Berri S. Theoretical analysis of the structural, electronic and optical properties of tetragonal  $\text{Sr}_2\text{GaSbO}_6$ . *Chinese Journal of Physics*. 2017; 55(6): 2476-2483. <https://doi.org/10.1016/j.cjph.2017.11.001>